THE JOURNAL OF PHYSICAL CHEMISTRY C

ARTICLE

pubs.acs.org/JPCC

# Joint Photophysical and Electrical Analyses on the Influence of Conjugation Order in D-$\pi$-A Photosensitizers of Mesoscopic Titania Solar Cells

Jingyuan Liu,[†,‡] Difei Zhou,[‡] Fangfang Wang,[‡] Francisco Fabregat-Santiago,[§] Sara G. Miralles,[§] Xiaoyan Jing,[*,†] Juan Bisquert,[*,§] and Peng Wang[*,‡]

[†]Key Laboratory of Superlight Materials and Surface Technology, College of Materials Science and Chemical Engineering, Harbin Engineering University, Harbin 150001, China

[‡]State Key Laboratory of Polymer Physics and Chemistry, Changchun Institute of Applied Chemistry, Chinese Academy of Sciences, Changchun 130022, China

[§]Photovoltaic and Optoelectronic Devices Group, Physics Department, Universitat Jaume I, 12071 Castello, Spain

Supporting Information

**ABSTRACT:** Diverse thiophene-containing blocks have been employed as the $\pi$-conjugated spacers of organic D-$\pi$-A dyes. In the case that multiple segments with distinguishable electronic features are applied, their conjugation sequence could potently affect optoelectric behaviors of photosensitizers in mesoscopic titania solar cells. In this work, we address this issue by designing three organic dyes (C225, C226, and C227), wherein the dihexyl-substituted cyclopentadithiophene moiety is stepwise shifted from the electron acceptor side to the donor one, along with the additional use of two 3-hexylthiophene rings as the conjugated spacing unit. With respect to C225 and C226, C227 presents a relatively inefficient photoinduced electron injection as indicated by photoluminescence measurements, which accounts for its lower efficiencies of converting incident monochromatic photons to collected electrons. Transient absorption measurements suggest that the charge recombination between oxidized dye molecules and titania electrons gradually decelerates from C225 to C227, while the interception of oxidized dye molecules by iodide ions exhibits an apparent driving force dependent, Marcus normal region behavior.

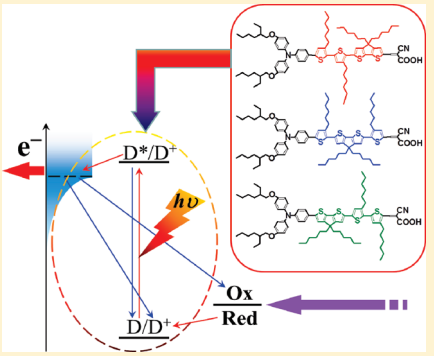


## 1. INTRODUCTION

In response to the urgent demand for massively scalable carbon-free energy sources, intensive efforts have been concentrated on both elevating the efficiency and lowering the cost of solar-to-electricity conversion.[1] During the past years dye-sensitized solar cells (DSCs)[2] have received an ever-increasing amount of research attention on account of their grand feasibility to supply sustainable and clean electricity based on resource-abundant raw materials and easy processing. In this photoelectrochemical device, light absorption by dye molecules anchored on a nanocrystalline titania film is intimately followed by electron injection into the accepting states of titania. To ensure an efficient charge collection, photogenerated carriers need to traverse through the micrometer-thick titania film to the current collector before intercepted by oxidized species. Material innovation and extensive device engineering have consecutively impelled the encouraging advancements of device performance in the foregone two decades. Thus far, the highest validated power conversion efficiency of 11.1%[3] at the AM 1.5G conditions has been achieved, by elaborately combining a panchromatic ruthenium sensitizer and an iodine electrolyte.

With a view to the resource limitation of ruthenium, much has been done to develop organic D-$\pi$-A photosensitizers in recent years,[4] primarily in virtue of the wide availability of raw materials. Moreover, the flexible molecular tailoring of metal-free dye molecules provides special opportunity to design powerful sensitizers, potently advancing the photovoltaic performance of organic DSCs.[4l] In a typical D-$\pi$-A dye, not only structural modifications of the electron donor/acceptor can affect the ultimate power output but a change of the $\pi$-conjugated block also confers effective modulation on both the properties of the molecule itself and the physicochemical characteristics of the titania/dye/electrolyte interface, which has immense effects on cell performance.[4b,f,5] In this context, $\pi$-conjugation extension has served as a popular strategy toward improving the light harvest capacity of a sensitizer. This tactic, on the other side, raises an important issue relevant to the elaboration of the conjugation block, i.e., the conjugating sequence of different conjugation segments. In this work, we investigate the possible

**Received:** April 9, 2011
**Published:** July 06, 2011

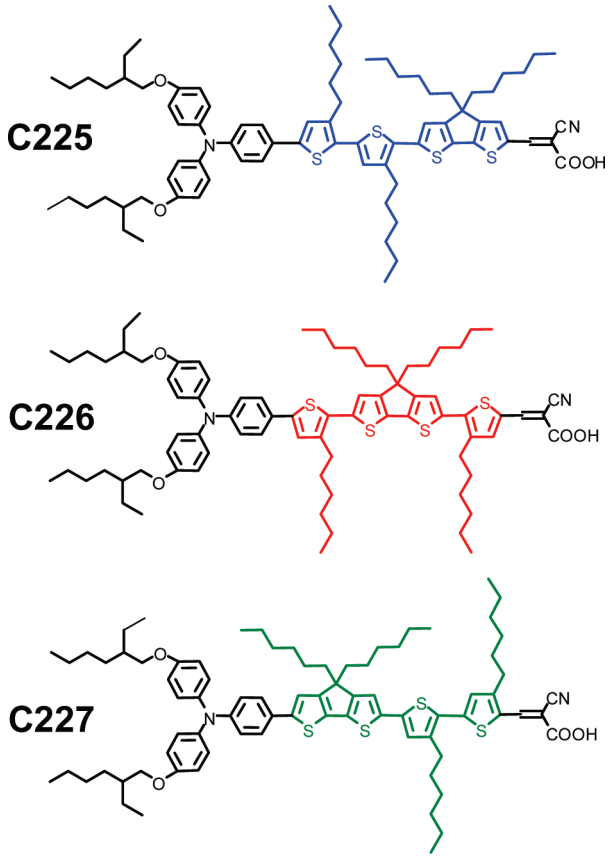


**Figure 1.** Molecular structures of dyes featuring different conjugation orders.

influence of $\pi$-conjugation order upon the optoelectronic characteristics of organic DSCs by designing three model organic dyes (C225, C226, and C227, Figure 1) with serially varied conjugation orders of a cyclopentadithiophene unit and two 3-hexylthiophene segments. Important photovoltaic features, such as incident photon-to-collected electron conversion efficiency (IPCE) and photovoltage, are scrutinized with a joint photophysical and electrochemical characterization.

## 2. EXPERIMENTAL SECTION

**2.1. Materials.** Solvents are distilled before use. Cyanoacetic acid, piperidine, 3α,7α-dihydroxy-5β-cholic acid (cheno), iodine ($I_2$), lithium iodide (LiI), lithium bis(trifluoromethanesulfonyl)-imide (LiTFSI), 4-*tert*-butylpyridine (TBP), and guanidinium thiocyanate (GNCS) were purchased from Aldrich. The scattering $TiO_2$ paste (WER2-O) was received as a gift from Dyesol. 1,3-Dimethylimidazolium iodide (DMII) and 1,3-dimethylimidazolium bis(trifluoromethanesulfonyl)imide (DMITFSI) were synthesized according to the literature methods.[6] $^1$H and $^{13}$C NMR spectra were recorded on a Bruker AV-400 MHz or AV-600 MHz instrument with tetramethylsilane as the internal standard. Mass spectra were performed through electrospray ionization on a Thermo LTQ XL. Elemental analyses were performed on GmbH VarioEL.

**2.2. Dye Preparation.** The synthetic routes and syntheses of intermediates of C225−C227 are detailed in the Supporting Information, and the general synthesis of dye molecules is presented as follows, using the Knoevenagel condensation reaction.

*General Procedure for the Synthesis of C225, C226, and C227 Sensitizers.* To a stirred solution of aldehyde **6**, **16**, or **24** (1 mmol) and cyanoacetic acid (3 mmol) in chloroform (30 mL) was added piperidine (7 mmol). The reaction mixture was refluxed under argon for 12 h and then acidified with 2 M hydrochloric acid aqueous solution (30 mL). The crude product was extracted into chloroform, washed with water, and dried over anhydrous sodium sulfate. After removing solvent under reduced pressure, the residue was purified by flash chromatography with toluene and toluene/methanol (10/1, v/v) in turn as eluent to yield a black powder.

*2-Cyano-3-{6-{5-{4-[N,N-bis(4-(2-ethylhexyloxy)phenyl)-amino]phenyl}-3,4′-dihexyl-[2,2′-bithiophen]-5′-yl}-4,4-dihexyl-4H-cyclopenta[2,1-b:3,4-b′]dithiophene-2-yl}acrylic Acid (**C225**).* Yield: 71%. $^1$H NMR (400 MHz, DMSO-$d_6$) $\delta$: 13.29 (s, 1H), 8.41 (s, 1H), 7.94 (s, 1H), 7.46 (d, $J$ = 8.4 Hz, 2H), 7.33 (s, 1H), 7.27 (s, 1H), 7.12 (s, 1H), 7.05 (d, $J$ = 8.8 Hz, 4H), 6.94 (d, $J$ = 8.8 Hz, 4H), 6.78 (d, $J$ = 8.4 Hz, 2H), 3.84 (d, $J$ = 5.6 Hz, 4H), 2.75 (m, 4H), 1.92 (m, 4H), 1.65 (m, 6H), 1.29 (m, 32H), 1.11 (m, 12H), 0.89 (m, 18H), 0.77 (t, $J$ = 7.0 Hz, 6H). $^{13}$C NMR (150 MHz, THF-$d_8$) $\delta$: 165.09, 161.01, 159.53, 157.45, 155.97, 149.77, 147.64, 145.37, 144.97, 143.87, 141.95, 140.04, 138.65, 137.36, 135.35, 130.91, 128.96, 128.61, 128.35, 127.84, 127.53, 127.02, 121.94, 120.42, 117.66, 117.41, 116.49, 98.37, 71.61, 68.38, 55.55, 41.14, 39.34, 33.14, 33.05, 33.02, 32.61, 32.05, 31.76, 31.41, 31.19, 31.11, 30.67, 30.56, 30.36, 29.96, 26.26, 25.30, 24.44, 24.01, 23.98, 23.93, 14.90, 14.85, 11.99. MS (ESI) $m/z$ calcd. for ($C_{79}H_{104}N_2O_4S_4$): 1272.7. Found: 1271.7 ([M−H]$^-$). Anal. Calcd. for $C_{79}H_{104}N_2O_4S_4$: C, 74.48; H, 8.23; N, 2.20. Found: C, 74.54; H, 8.17; N, 2.22.

*2-Cyano-3-{5-{6-{5-{4-[N,N-bis(4-(2-ethylhexyloxy)phenyl)-amino]phenyl}-3-hexylthiophene-2-yl}-4,4-dihexyl-4H-cyclopenta[2,1-b:3,4-b′]dithiophene-2-yl}-4-hexylthiophene-2--yl}-acrylic Acid (**C226**).* Yield: 71%. $^1$H NMR (400 MHz, DMSO-$d_6$) $\delta$: 13.29 (s, 1H), 8.40 (s, 1H), 7.91 (s, 1H), 7.46 (m, 3H), 7.27 (s, 1H), 7.21 (s, 1H), 7.04 (d, $J$ = 8.8 Hz, 4H), 6.94 (d, $J$ = 8.8 Hz, 4H), 6.77 (d, $J$ = 8.4 Hz, 2H), 3.84 (d, $J$ = 5.6 Hz, 4H), 2.83 (m, 2H), 2.76 (m, 2H), 1.95 (m, 4H), 1.64 (m, 6H), 1.29 (m, 32H), 1.11 (m, 12H), 0.90 (m, 18H), 0.77 (m, 6H). $^{13}$C NMR (150 MHz, THF-$d_8$) $\delta$: 164.64, 160.73, 159.75, 157.54, 150.04, 146.58, 143.63, 142.88, 141.87, 141.67, 141.01, 140.52, 139.83, 136.91, 136.12, 134.06, 130.75, 128.67, 128.02, 127.33, 127.24, 126.23, 123.41, 121.53, 121.18, 117.15, 116.51, 99.53, 71.61, 68.38, 55.73, 41.14, 39.08, 33.16, 33.10, 33.03, 32.05, 31.86, 31.37, 31.11, 31.06, 30.76, 30.73, 30.64, 30.56, 26.26, 26.13, 25.30, 24.44, 24.02, 23.99, 14.90, 14.86, 11.99. MS (ESI) $m/z$ calcd. for ($C_{79}H_{104}N_2O_4S_4$): 1272.7. Found: 1271.7 ([M−H]$^-$). Anal. Calcd. for $C_{76}H_{104}N_2O_4S_4$: C, 74.48; H, 8.23; N, 2.20. Found: C, 74.53; H, 8.205; N, 2.16.

*2-Cyano-3-{5-{5-{6-{4-[N,N-bis(4-(2-ethylhexyloxy)phenyl)-amino]phenyl}-4,4-dihexyl-4H-cyclopenta[2,1-b:3,4-b′]dithiophene-2-yl}-3-hexylthiophene-2-yl}-3-hexylthiophene-2-yl}-acrylic Acid (**C227**).* Yield: 73%. $^1$H NMR (400 MHz, DMSO-$d_6$) $\delta$: 13.29 (s, 1H), 8.30 (s, 1H), 7.48 (m, 3H), 7.39 (s, 1H), 7.33 (d, $J$ = 8.8 Hz, 2H), 7.02 (d, $J$ = 8.4 Hz, 4H), 6.93 (d, $J$ = 8.4 Hz, 4H), 6.79 (d, $J$ = 8.8 Hz, 2H), 3.84 (d, $J$ = 4.8 Hz, 4H), 2.82 (m, 4H), 1.88 (m, 4H), 1.64 (m, 6H), 1.30 (m, 32H), 1.11 (m, 12H), 0.90 (m, 18H), 0.77 (t, $J$ = 7.2 Hz, 6H). $^{13}$C NMR (150 MHz, THF-$d_8$) $\delta$: 164.13, 159.32, 157.56, 150.10, 149.48, 147.81, 143.99, 142.68, 142.13, 141.86, 141.83, 138.46, 136.96, 136.59, 132.61, 131.78, 129.78, 129.53, 128.42, 128.05, 127.28, 127.24, 126.20, 121.47, 121.35, 117.88, 116.51, 96.91, 71.61, 68.63, 55.43, 41.13, 38.99, 33.14, 32.98, 32.05, 31.85, 31.82,

31.05, 30.95, 30.93, 30.71, 30.64, 30.56, 26.26, 26.13, 25.30, 24.44, 24.02, 23.95, 14.91, 14.85, 12.00. MS (ESI) $m/z$ calcd. for ($C_{79}H_{104}N_2O_4S_4$): 1272.7. Found: 1271.7 ([M−H]$^-$). Anal. Calcd. for $C_{79}H_{104}N_2O_4S_4$: C, 74.48; H, 8.23; N, 2.20. Found: C, 74.41; H, 8.28; N, 2.27.

**2.3. Device Fabrication and Characterizations.** A bilayer titania film (7 + 6 $\mu$m thick) screen-printed on fluorine-doped tin oxide (FTO) conducting glass (Nippon Sheet Glass, Solar, 4 mm thick) was used as the negative electrode for cell fabrication. A transparent layer of 22-nm-sized $TiO_2$ particles (7 $\mu$m thick) was first printed on FTO glass and further coated with a 6-$\mu$m thick second layer of scattering titania particles (WER2-O, Dyesol). Preparation procedures of titania nanocrystals, paste for screen-printing, and nanostructured titania film were reported in a previous paper.[7] A circular $TiO_2$ electrode (~0.28 cm$^2$) was stained by immersing it into a dye solution containing C225, C226, or C227 (150 $\mu$M) and cheno (300 $\mu$M) in chlorobenzene for 5 h. After washing with acetonitrile and drying by air flow, the dye-coated titania electrode was assembled with a thermally platinized FTO electrode. The electrolyte for device fabrication is composed of 1.0 M DMII, 30 mM $I_2$, 50 mM LiI, 1.0 M TBP, and 0.1 M GNCS in acetonitrile. Details on cell assembling and characterizations are described in our previous publication.[8]

**2.4. Absorption and Emission Measurements.** Steady-state absorption spectra were recorded on a PerkinElmer Lamda 900 spectrometer. Transient absorption measurements were performed with a LP920 laser flash spectrometer pumped with a nanosecond tunable OPOLett-355II laser. The sample was kept at a 45° angle with respect to the excitation beam. Transient absorption spectra were measured with an intensified charge-coupled detector (ICCD) camera using a xenon arc lamp as probe light. In the kinetic measurements, the probe light passed through a bandpass filter (center wavelength = 782 nm) was dispersed by a monochromator before being detected by a fast photomultiplier tube and recorded with a TDS 3012C digital signal oscilloscope. Time-correlated single photon counting measurements were carried out on a LifeSpec-II spectrometer employing an EPL635 pulsed laser diode and a Hamamatsu H5773−04 photomultiplier.

**2.5. Electrochemical Measurements.** A CHI660C electrochemical workstation was used for voltammetric measurements. The measurements of the ground-state redox potentials of dyes were accomplished with a three-electrode electrochemical cell composed of a platinum gauze counter electrode, a Ag/AgCl (sat. KCl) reference electrode, and a working electrode of a dye-coated titania film on FTO. Impedance spectroscopies were recorded under various irradiations with a white light-emitting diode on an IM6ex electrochemical workstation, with a frequency range of 50 mHz−100 kHz and a potential modulation of 20 mV. A potential bias ($V$) was applied to equal the open-circuit photovoltage of the cell under each irradiation, fulfilling the criterion of a zero unmodulated current. The obtained impedance data were fitted with the Z-view software (v2.80, Scribner Associates Inc.) with a proper equivalent circuit adaptable to DSCs.[9,10]

## 3. RESULTS AND DISCUSSION

The light harvesting capacities of C225−C227 were first evaluated by measuring the electronic absorption spectra of diluted chloroform solutions, as presented in Figure 2A. Moving

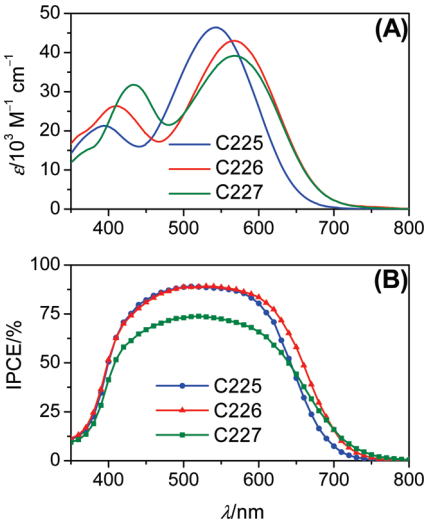


**Figure 2.** (A) Wavelength-dependent molar absorption coefficients derived from electronic absorption measurements of diluted chloroform solutions. (B) Photocurrent action spectra with an iodine electrolyte. Cells were tested using a metal mask with an aperture area of 0.158 cm$^2$. An antireflection film was adhered to the testing cell during measurement.

the cyclopentadithiophene moiety toward the triphenylamine side gradually decreases the maximum molar absorption coefficient from 4.65 × 10$^4$ to 4.30 × 10$^4$ and further to 3.92 × 10$^4$ M$^{-1}$ cm$^{-1}$, along with a 20-nm red-shift of the maximum absorption wavelength. We further measured the photocurrent action spectra of DSCs made from these dyes in conjunction with an iodine electrolyte, the composition of which can be found in the Experimental Section. As shown in Figure 2B, the onset wavelength of photocurrent response is stepwise red-shifted from C225 to C227, being in good agreement with the observation with electronic absorptions (Figure S1 of Supporting Information) of dye-coated titania films. Moreover, C225 and C226 confer the cells with comparable ~89% plateaus from 490 to 555 nm, while the utilization of the C227 dye brings forth a remarkably lower IPCE maximum of 74%.

The IPCE of a DSC is known as the accumulative contribution of wavelength-dependent efficiencies of light absorption of the photoactive layer and charge collection at the current collector, and wavelength-independent efficiency of net charge separation at the titania/dye interface. From Figure S1 of Supporting Information we can conclude that light absorption is saturated in the spectral coverage of 500−555 nm for the three cells based on C225−C227. Moreover, efficient collection of injected charges in these cells could be supported by comparing the electron diffusion lengths (Figure S2 of Supporting Information) derived from electrical impedance measurements, which were much larger than the titania film thickness used here. On the basis of these analyses, we can unambiguously ascribe the above IPCE height variation to the dye-dependent interfacial charge separation.

Transient absorption measurements were carried out to probe the dual-channel charge-transfer dynamics of oxidized dye molecules, i.e., the recombination of oxidized dye molecules with electrons back-transferred from titania and their interception by electron-donating iodide ions in electrolytes, the competition between which could be an important determinant of IPCE

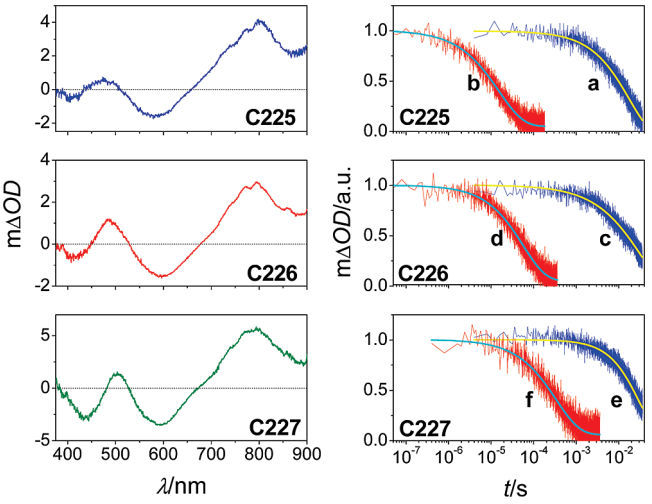


**Figure 3.** Transient absorption spectra (left) of 2.7-$\mu$m-thick, dye-coated titania films permeated with an inert electrolyte (1.0 M DMITF-SI, 50 mM LiTFSI, and 1.0 M TBP in acetonitrile) and kinetic absorption traces (right) of 9.0-$\mu$m-thick, dye-coated titania films with the inert (a, c, and e) and iodine (b, d, and f) electrolytes. Pulse fluence and excitation wavelength: a, 39.6 $\mu$J cm$^{-2}$ at 639 nm; b, 39.9 $\mu$J cm$^{-2}$ at 633 nm; c, 39.1 $\mu$J cm$^{-2}$ at 657 nm; d, 39.3 $\mu$J cm$^{-2}$ at 652 nm; e, 39.1 $\mu$J cm$^{-2}$ at 655 nm; f, 39.3 $\mu$J cm$^{-2}$ at 652 nm. Smooth lines are stretched exponential fittings over raw data obtained by averaging 800 laser shots.

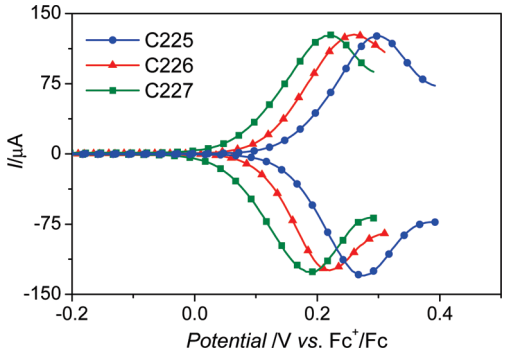


**Figure 4.** Square-wave voltammograms of dye-coated titania films. Supporting electrolyte: 0.1 M lithium bis(trifluoromethanesulfonyl)-imide. Scan rate: 50 mV s$^{-1}$.

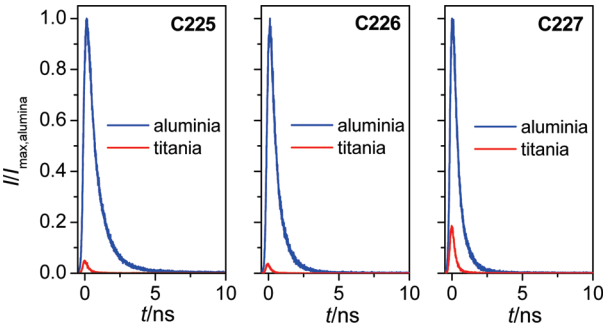


**Figure 5.** Time-correlated emission decay traces of dye-coated mesoporous alumina and titania films with an iodine electrolyte. Excitation wavelength: 639 nm. The emission intensity ($I$) was corrected in terms of the film absorbance at 639 nm and normalized with respect to the maximum emission intensity of the dye-coated alumina film ($I_{max,alumina}$).

height.[11] Before performing the kinetic measurements, we recorded the transient absorption difference spectrum (Figure 3) of a C225, C226, or C227 dye-coated titania film with an ICCD camera. While the broad negative signals in the visible region (C225, 510−657 nm; C226, 530−675 nm; C227, 528−670 nm) could be ascribed to the bleaching of ground-state dye molecules, the positive signals in the near-infrared regions were mainly attributed to the strong absorptions of oxidized dye molecules in comparison with their neutral counterparts. Note that we exclude any contribution from the emission of excited-state dye molecules to the transient signals, in virtue of our detection time at 3 $\mu$s upon laser excitation.

A monochromatic light at 782 nm was chosen to probe the dual-channel charge-transfer kinetics of oxidized dye molecules, on otherwise account of the sensitivity of the PMT detector of our measuring system. Excitation fluences were cautiously controlled in our measurements to guarantee that $\sim 1.26 \times 10^{14}$ photons cm$^{-2}$ were absorbed by the dye-coated titania films during every laser pulse. As shown in Figure 3, the kinetic traces could be well fitted to a stretched exponential decay function ($m\Delta OD \propto \exp[-(t/\tau)^{\alpha}]$), affording the half-lifetimes ($t_{1/2}$) of oxidized dye molecules. Upon utilizing an inert electrolyte containing the bis(trifluoromethanesulfonyl)imide anions, the transient absorption decays of oxidized C225−C227 dye molecules (traces a, c, and e) all display millisecond half-lifetimes (C225, 9.84 ms; C226, 15.8 ms; C227, 22.1 ms), indicative of fairly slow back electron transfer from titania to oxidized dye molecules. Furthermore, replacing the inert electrolyte with the realistic iodine electrolyte for cell fabrication evokes remarkably accelerated absorption decays (traces b, d, and f) with $t_{1/2}$ values of 11, 40, and 240 $\mu$s for C225, C226, and C227, respectively, arising from the expeditious electron donation from iodide ions to oxidized dye molecules. Apparently along with shifting the conjugated cyclopentadithiophene segment from cyanoacrylic acid electron-acceptor toward the triphenylamine electron-donor (from C225 to C227), a consecutive diminishment of the reaction rate of dye regeneration has been probed.

This scenario may be further understood in terms of a gradually negative shift of ground-state redox potential of dye molecule from C225 to C227 (C225, 0.29 V; C226, 0.24 V; C227, 0.21 V vs Fc$^+$/Fc), which can be derived from the square-wave voltammograms of dye-coated titania films shown in Figure 4. Moreover, this analysis also indicates that the dye regeneration reaction probably falls in the Marcus normal region.[12] Overall, albeit the apparent influence of conjugation order in the dye molecules upon the dual-channel charge-transfer dynamics of oxidized dye molecules, the kinetic branch ratios were over 90 for all our cells, suggesting that the oxidized dye molecules can be almost quantitatively regenerated. Thereby we conclude that the aforementioned IPCE maxima variation received negligible contribution from the differences between kinetic competition of oxidized dye molecules. Also note that lifetime of titania electrons obtained from impedance data as $\tau_n = R_{rec}C_{\mu}$ with $R_{rec}$ the recombination resistance, provides at 0.62 V (around maximum peak power) values of 160 ms for C225, 22 ms for C226, and 70 ms for C227, which are, by far, much longer than those of the reaction of dye regeneration. This result indicates that the electron losses in $TiO_2$ are dominated by the charge transfer to triiodide ions and not to oxidized dye molecules as expected for good cells.[13]

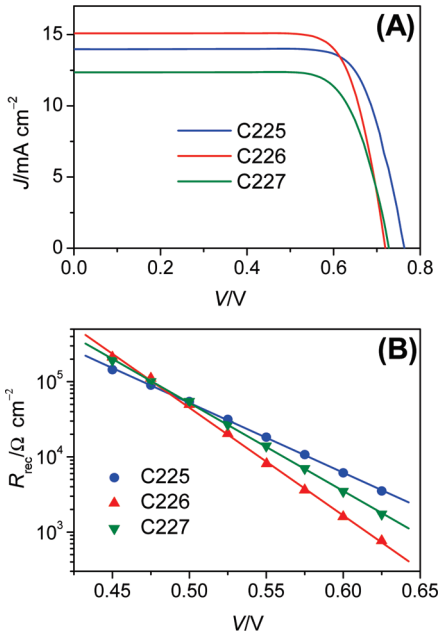


**Figure 6.** (A) $J-V$ characteristics of cells made with an iodine electrolyte measured under irradiation of 100 mW cm$^{-2}$ AM1.5 sunlight. The spectral distribution of our light resource simulates the AM1.5G solar emission (ASTM G173−03) with a mismatch less than 5%. Cells were tested using a metal mask with an aperture area of 0.158 cm$^2$. An antireflection film was adhered to the testing cell during measurement. (B) Charge recombination resistance of the iodine cells.

**Table 1. Photovoltaic Parameters Measured at the AM1.5 Full Sunlight Conditions**

| dye | $J_{sc}$ (mA cm$^{-2}$) | $V_{oc}$ (V) | FF | $\eta$ (%) |
|---|---|---|---|---|
| C225 | 14.0 | 0.77 | 0.77 | 8.3 |
| C226 | 15.1 | 0.72 | 0.78 | 8.4 |
| C227 | 12.3 | 0.73 | 0.76 | 6.9 |

Thereby we further resorted to the time-correlated single photon counting technique to scrutinize the possible effect of dissimilar conjugation order of organic dyes upon the yield ($\eta_{inj}$) of electron injection at the titania/dye interface, which can significantly impact the IPCE height.[14] A dummy cell was first fabricated by employing a C225, C226, or C227 dye-coated, 3-$\mu$m-thick alumina film impregnated with the realistic iodine electrolyte, exhibiting strong photoluminescence (blue lines in Figure 5) upon laser excitation at 639 nm. Considering the injection-prohibiting characteristics of the alumina/dye interface, we can assign these emission decays to the radiative and nonradiative deactivation of excited-state dye molecules. Further substituting alumina with nanocrystalline titania has strongly attenuated the photoluminescence intensity (red lines in Figure 5), suggesting the event of electron injection as an alternative nonradiative deactivation channel for excited-state sensitizers. By comparing the integral areas of emission traces of the dye-coated titania films with respect to the alumina counterparts, we estimated the electron injection yields of C225 and C226 cells to be ~97%, while the employment of the C227 dye prompted a remarkably lower $\eta_{inj}$ value of ~88%, which well substantiates the aforementioned IPCE maximum decline.

The photocurrent density−voltage ($J-V$) characteristics (Figure 6A) of cells made with C225−C227 in conjunction with the iodine electrolyte were measured at an irradiation of 100 mW cm$^{-2}$ with an AM1.5 sunlight simulator, and the detailed photovoltaic parameters were collected in Table 1. The short-circuit photocurrent densities ($J_{sc}$) of DSCs with C225, C226, and C227 are 14.0, 15.1, and 12.3 mA cm$^{-2}$, respectively, being in good agreement with integrals of the preceding IPCEs over the standard AM1.5G solar emission spectrum. While a change of $\pi$-conjugation order does not noticeably affect the fill factor (FF), C225 generates the highest open-circuit photovoltage ($V_{oc}$) of 0.77 V, contributing to a power conversion efficiency ($\eta$) of 8.3%. The $V_{oc}$ of the C226 and C227 cells are 0.72 and 0.73 V, making $\eta$ values of 8.4 and 6.9%, respectively. The values of $V_{oc}$ obtained may be qualitatively analyzed in terms of the recombination resistances[15] shown in Figure 6B: for potentials above 0.5 V, $R_{rec}$ presents increasing values for cells with C226, C227, and C225, leading to enhanced $V_{oc}$ despite the differences in $J_{sc}$. See Supporting Information for more details.

## 4. CONCLUSIONS

To summarize, by employing three organic D-$\pi$-A dyes (C225−C227) with serially varied conjugation order between a cyclopentadithiophene moiety and two 3-hexylthiophene units, we investigate the influence of different $\pi$-conjugation sequence upon the photovoltaic behaviors of organic dye-sensitized solar cells with an iodine electrolyte. The use of the C227 dye has generated a relatively lower yield of electron injection than its C225 and C226 counterparts, as proved by analyzing the transient emission spectroscopies. Moreover, transient absorption measurements indicate that the charge recombination between oxidized dye molecules and titania electrons is stepwise decelerated with the cyclopentadithiophene unit approaching the electron donor, along with an apparent Marcus-normal-region-behavior dye regeneration.

## ■ ASSOCIATED CONTENT

**Supporting Information.** Synthetic details of intermediates, additional spectral data, and analyses of apparent electron diffusion length and recombination resistance. This material is available free of charge via the Internet at http://pubs.acs.org.

## ■ AUTHOR INFORMATION

### Corresponding Author

*E-mail: jingxiaoyan@hrbeu.edu.cn (X.J.); bisquert@fca.uji.es (J.B.); peng.wang@ciac.jl.cn (P.W.).

## ■ ACKNOWLEDGMENT

The Chinese group thanks the National 973 Program (No. 2007CB936702 and No. 2011CBA00702), the National Science Foundation of China (No. 50973105 and No. 50773078), the CAS Knowledge Innovation Program (No. KGCX2-YW-326), the Key Scientific and Technological Program of Jilin Province (No. 10ZDGG012), and the CAS Hundred Talent Program for financial support. We are grateful to Dyesol for supplying the WER2-O scattering paste and to DuPont Packaging and Industrial Polymers for supplying the Bynel film. The Spanish group acknowledges financial support from Ministerio de Cíencia e Innovación under Projects HOPE CSD2007-00007 and MAT

2010-19827 and Generalitat Valenciana under Project PROMETEO/2009/058.

## REFERENCES

(1) Ardo, S.; Meyer, G. J. *Chem. Soc. Rev.* **2009**, *38*, 115.
(2) Grätzel, M. *Acc. Chem. Res.* **2009**, *42*, 1778.
(3) Chiba, Y.; Islam, A.; Watanabe, Y.; Komiya, R.; Koide, N.; Han, L. *Jpn. J. Appl. Phys.* **2006**, *45*, L638.
(4) For example, see:(a) Sayama, K.; Tsukagoshi, S.; Hara, K.; Ohga, Y.; Shinpou, A.; Abe, Y.; Suga, S.; Arakawa, H. *J. Phys. Chem. B* **2002**, *106*, 1363. (b) Horiuchi, T.; Miura, H.; Sumioka, K.; Uchida, S. *J. Am. Chem. Soc.* **2004**, *126*, 12218. (c) Kitamura, T.; Ikeda, M.; Shigaki, K.; Inoue, T.; Anderson, N. A.; Ai, X.; Lian, T.; Yanagida, S. *Chem. Mater.* **2004**, *16*, 1806. (d) Thomas, K. R. J.; Lin, J. T.; Hsu, Y.-C.; Ho, K.-C. *Chem. Commun.* **2005**, 4098. (e) Chen, Y.; Zeng, Z.; Li, C.; Wang, W.; Wang, X.; Zhang, B. *New J. Chem.* **2005**, *29*, 773. (f) Wang, Z.-S.; Koumura, N.; Cui, Y.; Takahashi, M.; Sekiguchi, H.; Mori, A.; Kubo, T.; Furube, A.; Hara, K. *Chem. Mater.* **2008**, *20*, 3993. (g) Qin, H.; Wenger, S.; Xu, M.; Gao, F.; Jing, X.; Wang, P.; Zakeeruddin, S. M.; Grätzel, M. *J. Am. Chem. Soc.* **2008**, *130*, 9202. (h) Li, Q.; Lu, L.; Zhong, C.; Shi, J.; Huang, Q.; Jin, X.; Peng, T.; Qin, J.; Li, Z. *J. Phys. Chem. B* **2009**, *113*, 14588. (i) Mishra, A.; Fischer, M. K. R.; Bäuerle, P. *Angew. Chem., Int. Ed.* **2009**, *48*, 2474. (j) Zhang, X.-H.; Cui, Y.; Katoh, R.; Koumura, N.; Hara, K. *J. Phys. Chem. C* **2010**, *114*, 18283. (k) Choi, H.; Raabe, I.; Kim, D.; Teocoli, F.; Kim, C.; Song, K.; Yum, J.-H.; Ko, J.; Nazeeruddin, M. K.; Grätzel, M. *Chem.—Eur. J.* **2010**, *16*, 1193. (l) Zeng, W.; Cao, Y.; Bai, Y.; Wang, Y.; Shi, Y.; Zhang, M.; Wang, F.; Pan, C.; Wang, P. *Chem. Mater.* **2010**, *22*, 1915.
(5) (a) Koumura, N.; Wang, Z.-S.; Mori, S.; Miyashita, M.; Suzuki, E.; Hara, K. *J. Am. Chem. Soc.* **2006**, *128*, 14256. (b) Tian, H.; Yang, X.; Chen, R.; Zhang, R.; Hagfeldt, A.; Sun, L. *J. Phys. Chem. C* **2008**, *112*, 11023. (c) Li, R.; Lv, X.; Shi, D.; Zhou, D.; Cheng, Y.; Zhang, G.; Wang, P. *J. Phys. Chem. C* **2009**, *113*, 7469. (d) Jiang, X.; Marinado, T.; Gabrielsson, E.; Hagberg, D. P.; Sun, L.; Hagfeldt, A. *J. Phys. Chem. C* **2010**, *114*, 2799. (e) Chen, C.-H.; Hsu, Y.-C.; Chou, H.-H.; Thomas, K. R. J.; Lin, J. T.; Hsu, C.-P. *Chem.—Eur. J.* **2010**, *16*, 3184.
(6) Bonhôte, P.; Dias, A.-P.; Papageorgiou, N.; Kalyanasundaram, K.; Grätzel, M. *Inorg. Chem.* **1996**, *35*, 1168.
(7) Wang, P.; Zakeeruddin, S. M.; Comte, P.; Charvet, R.; Humphry-Baker, R.; Grätzel, M. *J. Phys. Chem. B* **2003**, *107*, 14336.
(8) Liu, J.; Li, R.; Si, X.; Zhou, D.; Shi, Y.; Wang, Y.; Jing, X.; Wang, P. *Energy Environ. Sci.* **2010**, *3*, 1924.
(9) Bisquert, J. *J. Phys. Chem. B* **2002**, *106*, 325.
(10) Fabregat-Santiago, F.; Garcia-Belmonte, G.; Bisquert, J.; Zaban, A.; Salvador, P. *J. Phys. Chem. B* **2002**, *106*, 334.
(11) (a) Pelet, S.; Moser, J.-E.; Grätzel, M. *J. Phys. Chem. B* **2000**, *104*, 1791. (b) Reynal, A.; Forneli, A.; Palomares, E. *Energy Environ. Sci.* **2010**, *3*, 805.
(12) (a) Marcus, R. A.; Sutin, N. *Biochim. Biophys. Acta* **1985**, *811*, 265. (b) Clifford, J. N.; Palomares, E.; Nazeeruddin, M. K.; Grätzel, M.; Durrant, J. R. *J. Phys. Chem. C* **2007**, *111*, 6561.
(13) Green, A. N. M.; Palomares, E.; Haque, S. A.; Kroon, J. M.; Durrant, J. R. *J. Phys. Chem. B* **2005**, *109*, 12525.
(14) (a) Tachibana, Y.; Moser, J. E.; Grätzel, M.; Klug, D. R.; Durrant, J. R. *J. Phys. Chem.* **1996**, *100*, 20056. (b) Koops, S. E.; O' Regan, B. C.; Barnes, P. R. F.; Durrant, J. R. *J. Am. Chem. Soc.* **2009**, *131*, 4808.
(15) Barea, E. M.; Zafer, C.; Gultekin, B.; Aydin, B.; Koyuncu, S.; Icli, S.; Fabregat Santiago, F.; Bisquert, J. *J. Phys. Chem. C* **2010**, *114*, 19840.